

Supplementary Information for

Facile formation of barium titanium oxyhydride on a titanium hydride surface as an ammonia synthesis catalyst

Yoshihiro Goto,^{*a} Masashi Kikugawa,^a Keisuke Kobayashi,^b Yuichi Manaka,^b Tetsuya Nanba,^b Hideyuki Matsumoto,^{b,c} Mitsuru Matsumoto,^a Masakazu Aoki,^a and Haruo Imagawa^a

^a Toyota Central R&D Labs., Inc., 41-1 Yokomichi, Nagakute, Aichi 480-1192, Japan.

^b Renewable Energy Research Center, National Institute of Advanced Industrial Science and Technology, 2-2-9 Machiikedai, Koriyama, Fukushima 963-0298, Japan.

^c Department of Chemical Science and Engineering, School of Materials and Chemical Technology, Tokyo Institute of Technology, 2-12-1 Ookayama, Meguro-ku, Tokyo, 152-8552, Japan.

1. Supplementary figures

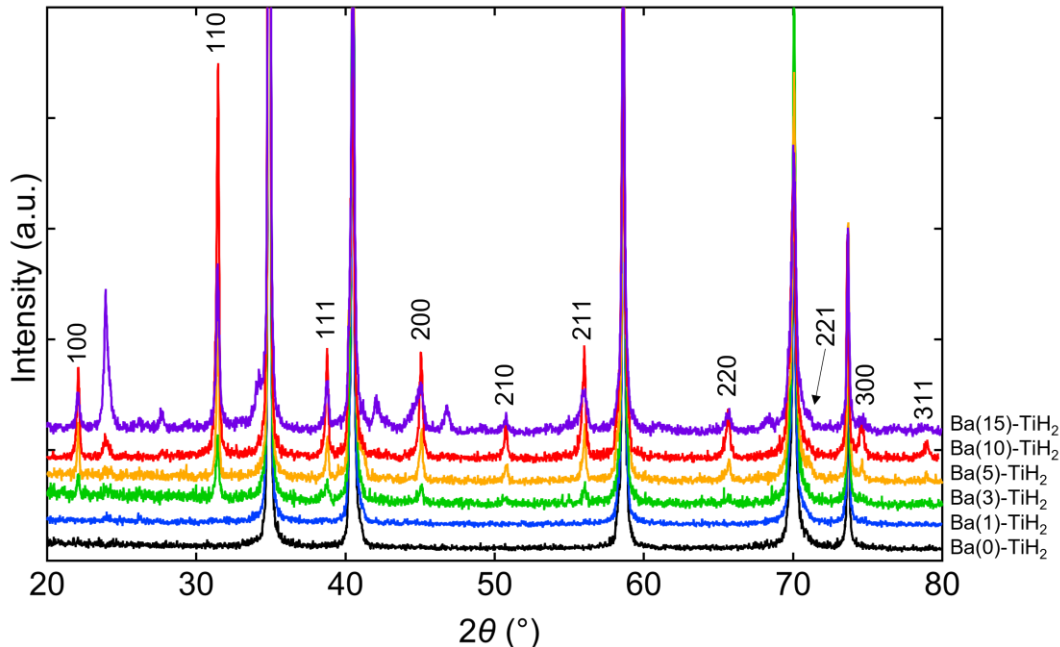


Fig. S1. Expanded XRD patterns of Ba(α)-TiH₂ ($\alpha = 0, 1, 3, 5, 10$, and 15) with Bragg reflections attributed to BaTiO_{2.5}H_{0.5}.

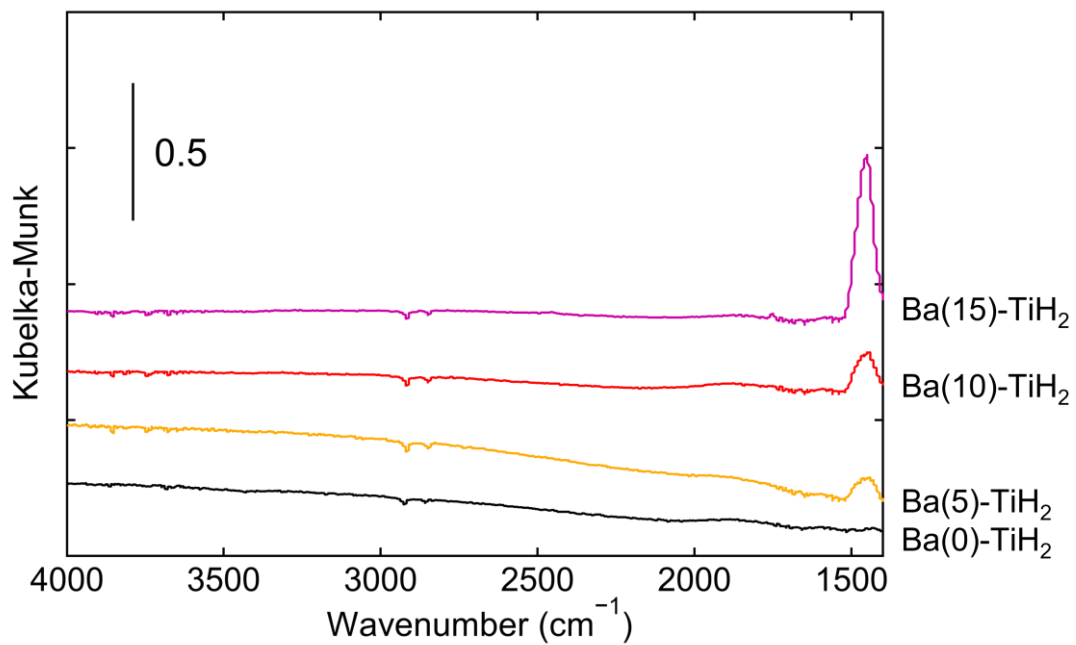


Fig. S2. FT-IR spectra of Ba(α)-TiH₂ ($\alpha = 0, 5, 10$, and 15) at $50\text{ }^{\circ}\text{C}$ in flowing He. Samples were pretreated at $200\text{ }^{\circ}\text{C}$ for 40 min in flowing He prior to analysis. Peaks at around 1450 cm^{-1} are assigned to the CO₃²⁻ ions of BaCO₃.^{S1}

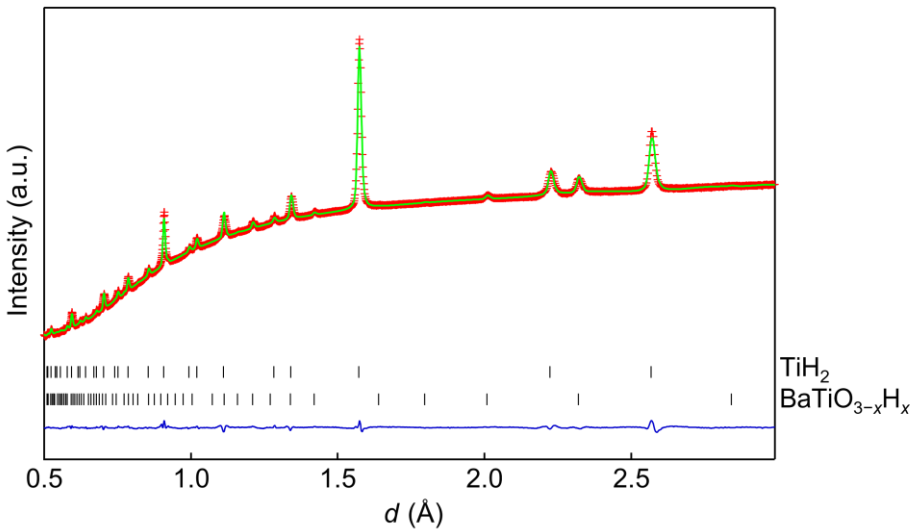


Fig. S3. Rietveld refinement profile for the ND pattern of Ba(10)-TiH₂. The red crosses, green solid line, and blue solid line correspond to observed and calculated intensities and their differences, respectively. The black ticks highlight the positions of the peaks corresponding to TiH₂ and BaTiO_{3-x}H_x.

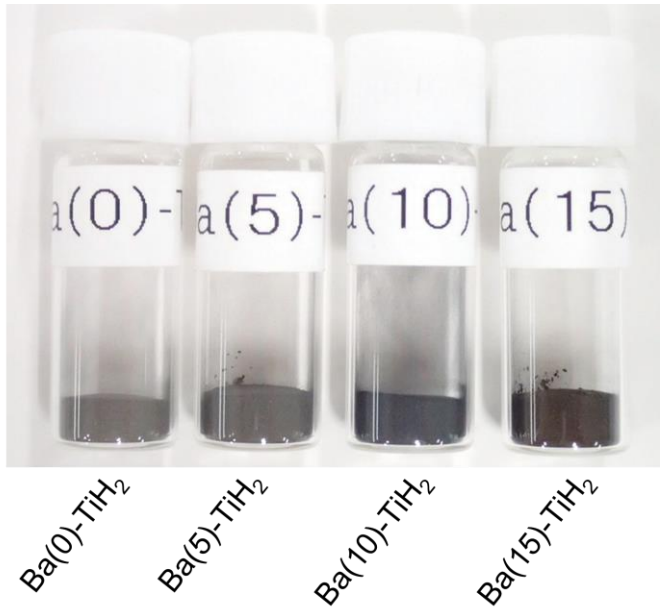


Fig. S4. Color changes accompanying the formation of $\text{BaTiO}_{2.5}\text{H}_{0.5}$ and BaCO_3 on the TiH_2 surface.

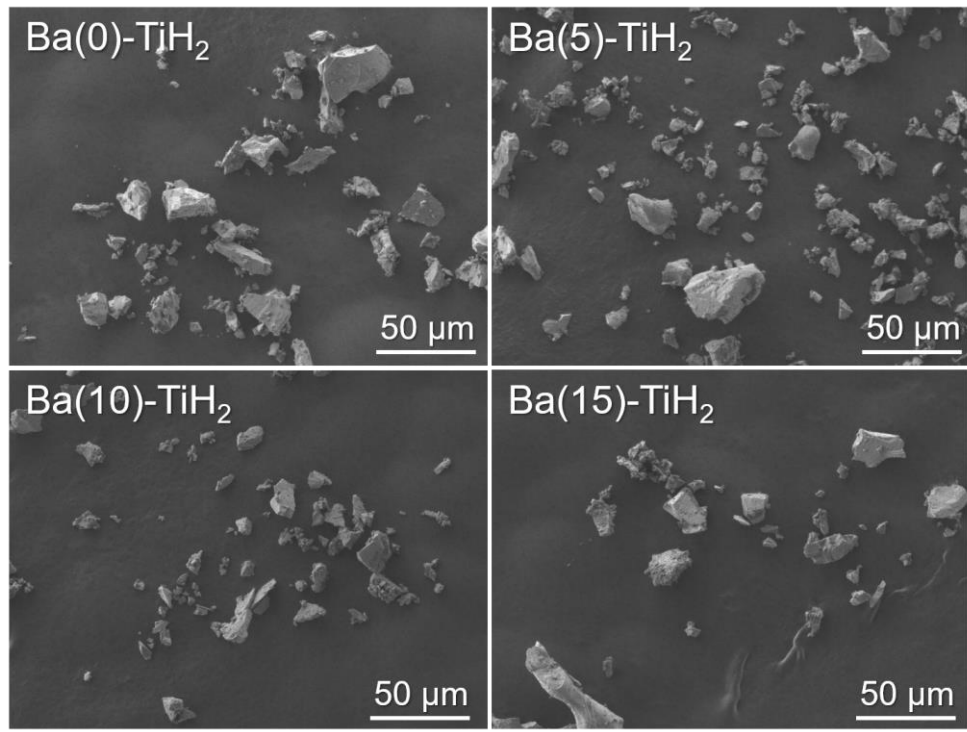


Fig. S5. Scanning electron microscopy (SEM) images of $\text{Ba}(\alpha)\text{-TiH}_2$ ($\alpha = 0, 5, 10$, and 15) at $500\times$ magnification.

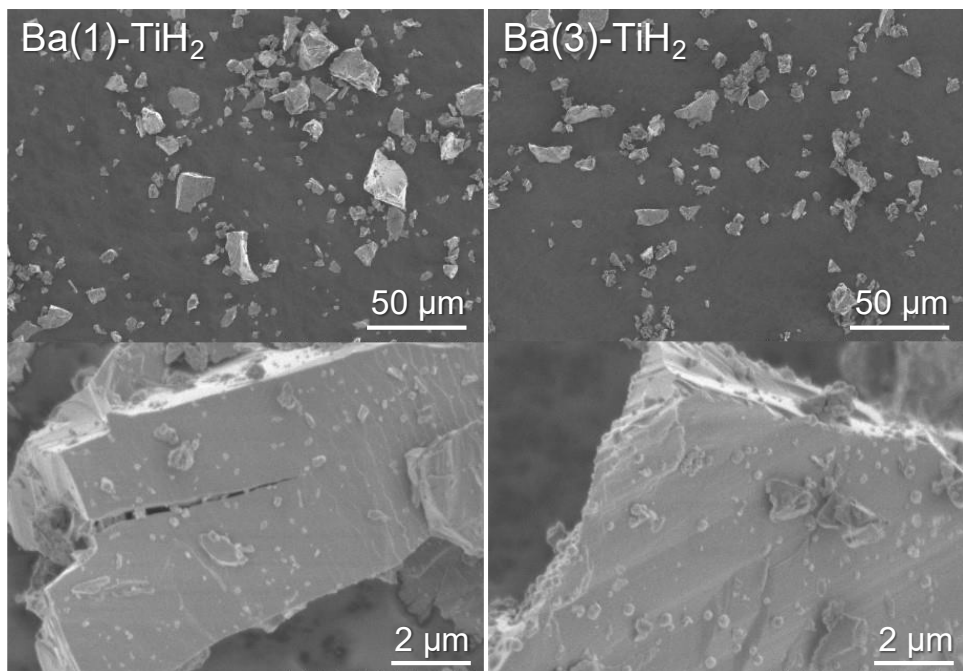


Fig. S6. Scanning electron microscopy (SEM) images of Ba(α)-TiH₂ (α = 1 and 3) at 500 \times and 10000 \times magnifications.

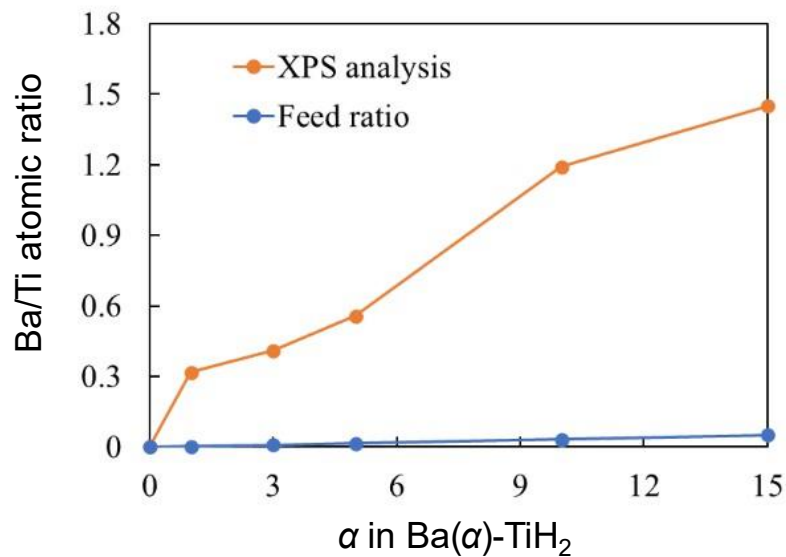


Fig. S7. Ba/Ti atomic ratio of $\text{Ba}(\alpha)\text{-TiH}_2$ ($\alpha = 0, 1, 3, 5, 10$, and 15) estimated from XPS analysis and the feed ratio.

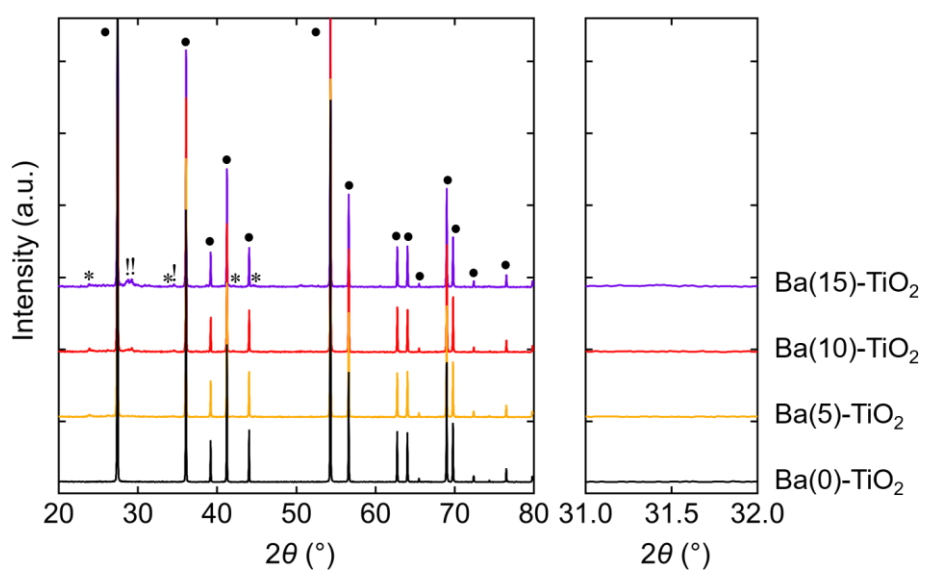


Fig. S8. XRD patterns of Ba(α)-TiO₂ ($\alpha = 0, 5, 10$, and 15). Circles (●), exclamation marks (!), and asterisks (*) indicate peaks arising from rutile TiO₂, Ba₂TiO₄, and BaCO₃, respectively.

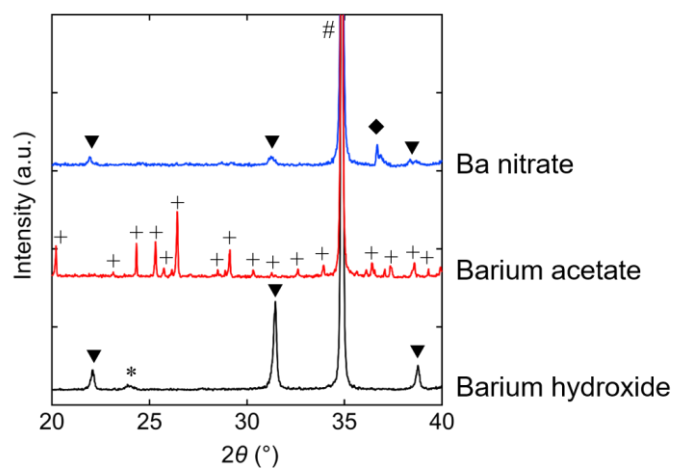


Fig. S9. XRD patterns of Ba(10)-TiH₂ prepared from various barium reagents. Hashtags (#), triangles (▼), asterisks (*), pluses (+), and squares indicate peaks arising from TiH₂, BaTiO_{2.5}H_{0.5}, BaCO₃, Ba(CH₃COO)₂, and Ba(NO₃)₂, respectively.

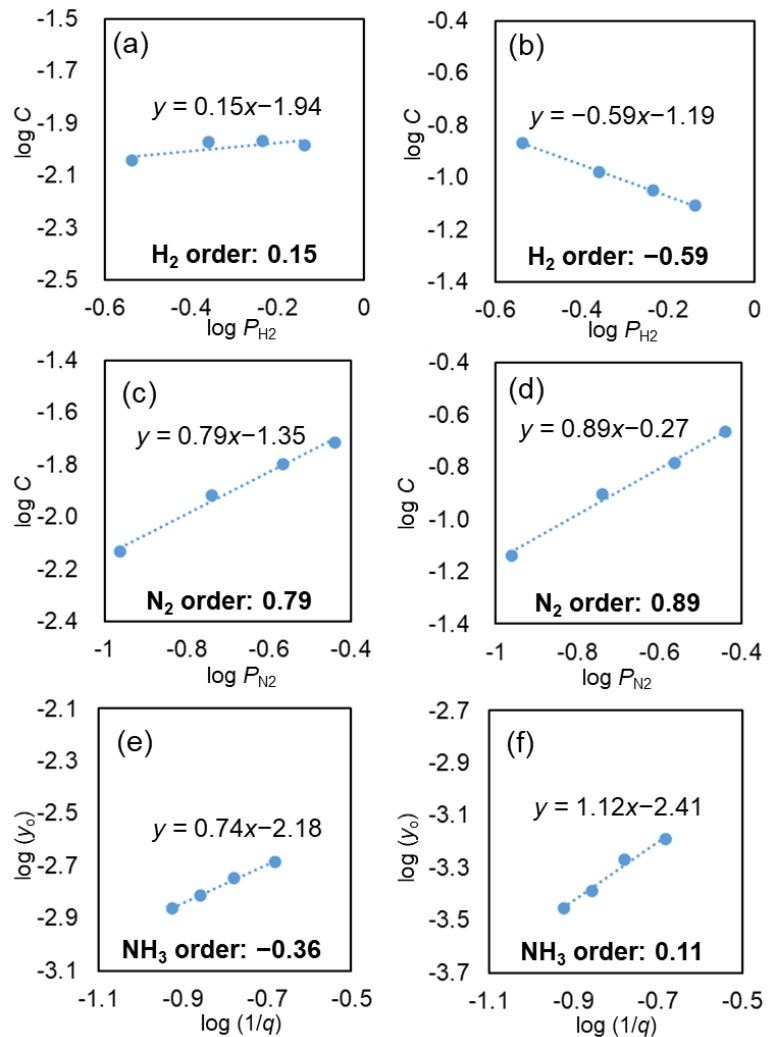


Fig. S10. Dependence of H_2 partial pressure (a, b), N_2 partial pressure (c, d), and flow rate (e, f) on the ammonia synthesis rates of Ru/Ba(10)- TiH_2 (a, c, e) and Ru-Cs/MgO (b, d, f) at 350 °C and 0.1 MPa. The reaction orders of the ammonia synthesis reaction were determined by the method reported by Aika et al.^{S2}

3. Supplementary tables

Table S1. Structural data for $\text{BaTiO}_{3-x}\text{H}_x$ ^a in Ba(10)-TiH₂ obtained by the Rietveld refinement of the neutron diffraction pattern.

Atom	Site	<i>g</i>	<i>x</i>	<i>y</i>	<i>z</i>	<i>U</i> _{iso} (Å ²)
Ba	1 <i>a</i>	1	0	0	0	0.0050(6)
Ti	1 <i>b</i>	1	0.5	0.5	0.5	0.0050(6)
O	3 <i>c</i>	0.886(2)	0	0.5	0.5	0.0079(5)
H	3 <i>c</i>	0.114(2)	0	0.5	0.5	0.0079(5)

^a Space group *Pm-3m* (No. 221), *a* = 4.01659(8) Å, *R*_{wp} = 0.7173%, *R*_p = 0.5601%, *S* = 4.9372.

Table S2. Elemental composition of Ba(α)-TiH₂ (α = 0, 1, 3, 5, 10, and 15) estimated from XPS analysis.

Sample	Ba (3d ₅)	Ti (2p)	O (1s)
Ba(0)-TiH ₂	0	32.21	67.79
Ba(1)-TiH ₂	6.99	22.01	71.01
Ba(3)-TiH ₂	9.06	22.05	68.88
Ba(5)-TiH ₂	11.26	20.23	68.51
Ba(10)-TiH ₂	17.87	15.00	67.13
Ba(15)-TiH ₂	19.57	13.50	66.93

Table S3. Reaction conditions^a and ammonia synthesis rates for kinetic analysis.

Reaction order	H ₂ /N ₂ ratio	Flow rate (mL min ⁻¹)				NH ₃ synthesis rate (mmol g ⁻¹ h ⁻¹)	
		H ₂	N ₂	Ar	Total	Ru/Ba(10)-TiH ₂	Ru-Cs/MgO
H ₂	2	32	16	62	110	0.87	0.24
	3	48	16	46	110	0.98	0.18
	4	64	16	30	110	0.99	0.15
	5	80	16	14	110	0.96	0.13
N ₂	5	60	12	38	110	0.75	0.12
	3	60	20	30	110	1.08	0.22
	2	60	30	20	110	1.32	0.30
	1.5	60	40	10	110	1.52	0.41
NH ₃	3	48	16	16	80	1.34	0.21
	3	60	20	20	100	1.46	0.22
	3	72	24	24	120	1.50	0.20
	3	84	28	28	140	1.56	0.20

^a All data were collected at 350 °C and atmospheric pressure.

4. References

- S1 E. Roedel, A. Urakawa, S. Kureti and A. Baiker, *Phys. Chem. Chem. Phys.*, 2008, **10**, 6190.
S2 K. Aika, M. Kumasaka, T. Oma, O. Kato, H. Matsuda, N. Watanabe, K. Yamazaki, A. Ozaki and T. Onishi, *Appl. Catal.* 1986, **28**, 57.